# Experimental and mathematical characterisation of the rheological instability of concentrated waste activated sludge subject to anaerobic digestion

Wei, Peng; Tan, Qiuman; Uijttewaal, Wim; van Lier, Jules B.; de Kreuk, Merle

**DOI**
10.1016/j.cej.2018.04.108

**Publication date**
2018

**Document Version**
Final published version

**Published in**
Chemical Engineering Journal

Chemical Engineering Journal 349 (2018) 318–326

Contents lists available at ScienceDirect

# Chemical Engineering Journal

journal homepage: www.elsevier.com/locate/cej

# Experimental and mathematical characterisation of the rheological instability of concentrated waste activated sludge subject to anaerobic digestion

Peng Wei[a,*], Qiuman Tan[a], Wim Uijttewaal[b], Jules B. van Lier[a], Merle de Kreuk[a]

[a] Delft University of Technology, Department of Water Management, Stevinweg 1, 2628 CN Delft, The Netherlands
[b] Delft University of Technology, Department of Hydraulic Engineering, Stevinweg 1, 2628 CN Delft, The Netherlands

## HIGHLIGHTS

- Yield-pseudoplastic behaviour with varying patterns in a wide shear rate range.
- Improved characterisation by hybrid model fitting of defined shear rate segments.
- Rheological model fitting reflected transient status but not intrinsic properties.
- TS-related distinct flow status and transitions described rheological instability.
- Measurement recommendations and a mathematical expression for sludge rheology.

## ARTICLE INFO

*Keywords:*
Waste activated sludge
Rheological instability
Model fitting
Yield-pseudoplastic
Thixotropy

## ABSTRACT

For a proper operational performance assessment of excess sewage sludge digesters in practice, a better understanding of waste activated sludge (WAS) rheological behaviour is important, especially regarding the low-shear and poor mixing zones in anaerobic digesters. The potential rheological instability of WAS with different total solids (TS) concentrations was studied in this research. The obtained yield-pseudoplastic behaviour showed varying patterns in a wide shear rate range, of which characterisation depended on hybrid model fitting of defined shear rate segments. Although a new mathematical expression improved the fitting quality, limited applicability of the empiric models reflected the samples' transient rheological behaviour rather than intrinsic properties, challenging the included parameters definition. Characterised by the distinct flow status and transitions, the observed rheological instability gives more insight in viscoelastic and thixotropic effects on sludge flow and mixing behaviour in full-scale WAS treatment systems. Recommendations for developing a rheological measurement protocol were also formulated.

## 1. Introduction

Waste activated sludge (WAS) is a complex matrix, diverse and sensitive to origin and condition during transportation, processing and anaerobic digestion [1,2]. Although crucial for energy input assessments and operational optimisation of mixing in anaerobic digesters at wastewater treatment plants (WWTP), the rheology of thickened WAS is still not fully understood.

Rheological behaviour can differ with the different existing sludge types and can be affected by various factors. Although non-Newtonian behaviour (shear-thinning) was found for activated sludge (AS) in several studies [3–5], it has also been reported that AS with low total solids (TS) concentrations ($< 1\%$) has a relatively constant apparent viscosity with yield stress [5,6]. Sludge with higher TS has generally been found as yield-pseudoplastic (or viscoplastic) [7]; whereas the specific behaviour can be quite different in sludge types [8–12]. So solids content has been found to strongly affect the sludge rheology, including AS [3–6,13–15], primary and secondary sludge [5,11,16], and the mixture of those two [5,9,11,12,16]. The interactions of solid particles and the ambient fluid, including hydrodynamic and non-hydrodynamic parameters, were reported to play a major role in the rheological behaviour [15,17,18]. Moreover, the sludge rheology has been found to vary with operational conditions at the WWTP, such as sludge age and/or loading rate [19], flocculation [14,20], and aeration gas flow rate [4,19]. These operational parameters result in a diversity of sludge types with quite different physicochemical characteristics

* Corresponding author at: PO Box 5048, 2600 GA Delft, The Netherlands.
*E-mail address:* p.wei@tudelft.nl (P. Wei).

https://doi.org/10.1016/j.cej.2018.04.108
Received 10 February 2018; Received in revised form 13 April 2018; Accepted 17 April 2018
Available online 18 April 2018

**Nomenclature**

| | |
|---|---|
| d | gap width between measuring bob and cup of rheometer, m |
| $d_{eff}$ | width of localised shear layer, m |
| GT | gravitational thickened |
| K | flow consistency index, Pa·s$^n$ |
| $K_n$ | adjusted K, Pa$^{1/2}$·s$^{n/2}$ |
| m | rate constant in Cross model |
| n | flow behaviour index, −: fluid is shear-thinning if n < 1, Newtonian if n = 1, and shear-thickening if n > 1 |
| $R_i$ | the radius of measuring bob, m |
| $R_o$ | the radius of measuring cup, m |
| Re | Reynolds number, − |
| RMSE | root mean squared error, − |
| SSE | sum of squared errors, − |
| Ta | Taylor number, − |
| TS | total solids, % |
| VFC | vacuum-filtration-concentrated |
| WWTP | wastewater treatment plant |

*Greek symbols*

| | |
|---|---|
| $\dot{\gamma}$ | shear rate, s$^{-1}$ |
| $\dot{\gamma}_{eff}$ | effective shear rate of localised shear layer, s$^{-1}$ |
| $\lambda_{Ca}$ | time coefficient in Carreau model, s |
| $\lambda_{Cr}$ | time coefficient in Cross model, s$^m$ |
| μ | apparent viscosity, Pa·s |
| $\mu_0$ | zero-shear viscosity, Pa·s |
| $\mu_\infty$ | infinite rate apparent viscosity, Pa·s |
| υ | kinematic viscosity, m$^2$/s |
| τ | shear stress, Pa |
| $\tau_0$ | yield stress, Pa |
| $\tau_{1/2}$ | the critical shear stress in Ellis model, Pa |
| $\tau_C$ | the critical shear stress in the new expression, Pa |
| ω | angular velocity, rad/s |

[5,8]. Conductivity and pH were reported to affect the rheology as well [14]. In addition, thixotropy was investigated in some studies, whereas the observed time-dependent rheological behaviour was not further analysed [11,17].

The rheology of non-Newtonian fluids is usually described by applying mathematical rheological models based on curve-fitting empirical correlation expressions [21]. Typical models are shown in Table 1, including shear stress models and apparent viscosity models with different degrees of complexity. For sludge matrices, the Bingham model is usually found to fit the rheograms of AS well [5,6,13], while the Ostwald (or power-law) model [4,5,8,22,23] and the Herschel-Bulkley model [9,16,17,23] are found for thickened WAS (> 1%) better. There are also a few applications of other models for describing the sludge rheology, such as the Sisko model [3] and the Cross model [24]. Furthermore, mathematical expressions have been developed to further correlate some key influencing factors; exponential [3,6,11,12], power [11] and linear [9,11] relations have been reported to correlate the rheological properties towards the solids content.

In spite of the wide use, applicability of the models in Table 1 is specific to one sludge type or measuring condition, while usually the steady flow status at relatively high shear rates (> 10 s$^{-1}$) is used. The diverse and even contradictory results published, suggest that rheological characteristics of sludge might be too complicated to be described by a single rheological model containing empiric parameters. Moreover, there is a risk to apply one mathematical relation at different shear rates, since varying rheological behaviour has been reported at different shear rates [11,17,25]. In full scale sludge treatment installations, the WAS faces changing shear rates throughout the process: from high-shear-level pumping systems to low-shear-level anaerobic digesters, especially in the poor-mixed or dead zones where shear rates can go down towards 0 s$^{-1}$. Regarding considerable viscoelasticity observed in the untreated concentrated WAS [26], when the sludge with viscoelasticity and maybe thixotropy experiences medium and low shear rates, a good understanding of the potential instable and transitional rheological behaviour becomes important to assess sludge flow and mixing in full scale digesters. Nevertheless, this rheological instability has hardly been reported in literature.

In this study, the rheology of thickened WAS with different TS concentrations was measured and assessed in a wide shear rate range; particular attention was given to the low-shear regime in practice to investigate any rheological instability related to viscoelasticity and/or thixotropy.

## 2. Materials and methods

### 2.1. Sample characterisation

Excess secondary sewage sludge, sampled after gravitational thickening before feeding into an anaerobic digester at WWTP De Groote Lucht (Vlaardingen, the Netherlands), was used for this study. Considering the solids content impact, the sampled gravitational thickened (GT) sludge (of 1–2% TS) was concentrated by vacuum filtration to different TS concentrations up to 7%. In agreement with literature, the vacuum filtration was used in order to minimise any changes in the physical sludge structure [11]. All the GT and vacuum-filtration-concentrated (VFC) samples were stored at 4 °C and were tested within four days. The solids content was determined by standard gravimetric analysis, TS and volatile solids (VS) analysis following standard methods [27].

### 2.2. Rheological measurements

The rheology was measured using an Anton Paar MCR 302 Rheometer (Anton Paar GmbH, Austria), which has two concentric cylinders (measuring bob and cup) as a rotational Couette geometry. A CC27 measuring system was applied so the radii of the measuring bob and cup are 13.332 mm and 14.466 mm, respectively.

**Table 1**
Commonly used rheological models.

| Model | Expression | | Description |
|---|---|---|---|
| Bingham | $\tau = \tau_0 + \mu\dot{\gamma}$ | (1) | Constant viscosity with yield stress $\tau_0$ |
| Ostwald (de Waele) | $\tau = K\dot{\gamma}^n$ | (2) | Power law |
| Herschel-Bulkley | $\tau = \tau_0 + K\dot{\gamma}^n$ | (3) | Power law with $\tau_0$ |
| Casson | $\sqrt{\tau} = \sqrt{\tau_0} + \sqrt{\mu_\infty\dot{\gamma}}$ | (4) | With $\tau_0$ and limiting apparent viscosity $\mu_\infty$ |
| Sisko | $\mu = \mu_\infty + K\dot{\gamma}^{n-1}$ | (5) | Power law coupled with $\mu_\infty$ |
| Cross | $\frac{\mu-\mu_\infty}{\mu_0-\mu_\infty} = \frac{1}{1+\lambda_{Cr}\dot{\gamma}^m}$ | (6) | Four parameters including limiting apparent viscosities of $\mu_0$ and $\mu_\infty$ |
| Carreau | $\frac{\mu-\mu_\infty}{\mu_0-\mu_\infty} = (1+(\lambda_{Ca}\dot{\gamma})^2)^{\frac{n-1}{2}}$ | (7) | Four parameters including $\mu_0$ and $\mu_\infty$ |
| Ellis | $\mu = \frac{\mu_0}{1+(\tau/\tau_{1/2})^{\alpha-1}}$ | (8) | Function of shear stress, with a critical shear stress $\tau_{1/2}$ |

*2.2.1. Flow curve*

The flow curve measurement started with a pre-shear step of 90 s at a constant shear rate (generally 1000 $min^{-1}$), to minimise concentration gradients and to reach a homogeneous sample distribution. After a pause of 60 s, a flow measurement step in ramp mode was followed: the applied shear rate was increased from 0.01 $s^{-1}$ to 1000 $s^{-1}$, with a decreasing corresponding time interval, both of which varied logarithmically.

*2.2.2. Yield stress*

Two methods were applied for yield stress measurements. In method 1, the pre-shear and subsequent steps were similar to 2.2.1. The measuring step was in a torque ramp mode, and the torque imposed on the sample increased gradually from a value below the yielding process, of which the critical moment was determined by monitoring the responsive deflection angle. The second method was in a dynamic oscillation mode by using a PP50 plate system. The sample was in oscillation with a fixed frequency of 1 Hz and varying strains from 0.01 to 200%, and storage modulus and loss modulus were measured to determine yield stress.

*2.2.3. Creep test*

In order to further investigate rheological instability and thixotropy, a creep mode measurement was performed. In each sample test, constant shear stress in series with a duration of 106 s was applied. A shear stress range was set based on relevant flow curve results. Hence, the applied stress started below the yield stress and was successively increased up to the maximum shear rate (e.g. 1000 $s^{-1}$).

Triplicate measurements were typically performed for each sample. A constant temperature at 20 °C was controlled for all experiments, with a tolerance of ± 0.05 °C. No apparent stratification was observed when samples were kept static in containers for at least 3 h. Therefore, the influence of sludge settling during the duration of the experiments (maximum 20 min) was considered negligible.

## 3. Results and discussion

*3.1. Varying trends in flow curves*

Rheograms of the GT and the VFC sludge with TS concentrations of 1.2%, 3.6% and 6.0%, are shown in Fig. 1. All samples were found to show yielding and shear-thinning (or yield-pseudoplastic) behaviour, and returned flow curves with varying trends. For the GT sludge (TS 1.2%), the shear stress generally increased with the shear rate slightly at low shear rates, while had a faster increase above 12 $s^{-1}$ (Fig. 1A). For the VFC sludge (Fig. 1B and C), the rheogram showed two different segments of increasing shear stress (shear stress 2 and shear stress 3 in the graph), with a transition when the shear rate was around 10 $s^{-1}$. The VFC sludge also showed a decreasing shear stress part with the increasing shear rate at very low shear rates (usually < 0.3 $s^{-1}$), which has not been reported before for secondary sewage sludge [8,9,11,12].

All apparent viscosity and shear stress curves could be divided into three segments of similar behaviour, to better describe the varying trends in the wide shear rate range. For the GT sludge (Fig. 1A), the three segments were identified at shear rates 0.01–12, 12–350 and 350–1000 $s^{-1}$, respectively. For the VFC sludge (Fig. 1B and C), the first segment was the initial decreasing part of the shear stress curve, and the other two got distinct increasing trends.

*3.2. Mathematical characterisation on the varying trends*

*3.2.1. The Ostwald model and the Herschel-Bulkley model*

Mathematical characterisation on applicability of the segmentation for the varying trends in the rheograms was carried out using various rheological models. The most widely used models, the Ostwald model (Eq. (2)) and the Herschel-Bulkley model (Eq. (3)) were considered for both the whole curve and the defined segments, while the fitting quality was assessed by the sum of squared errors (SSE) and the root mean squared error (RMSE).

Results are presented in Fig. 1 and Table 2. Fitting of the full curves by both models gave unacceptable deviations (large SSE and RMSE values), but fitting each segment separately returned better results.

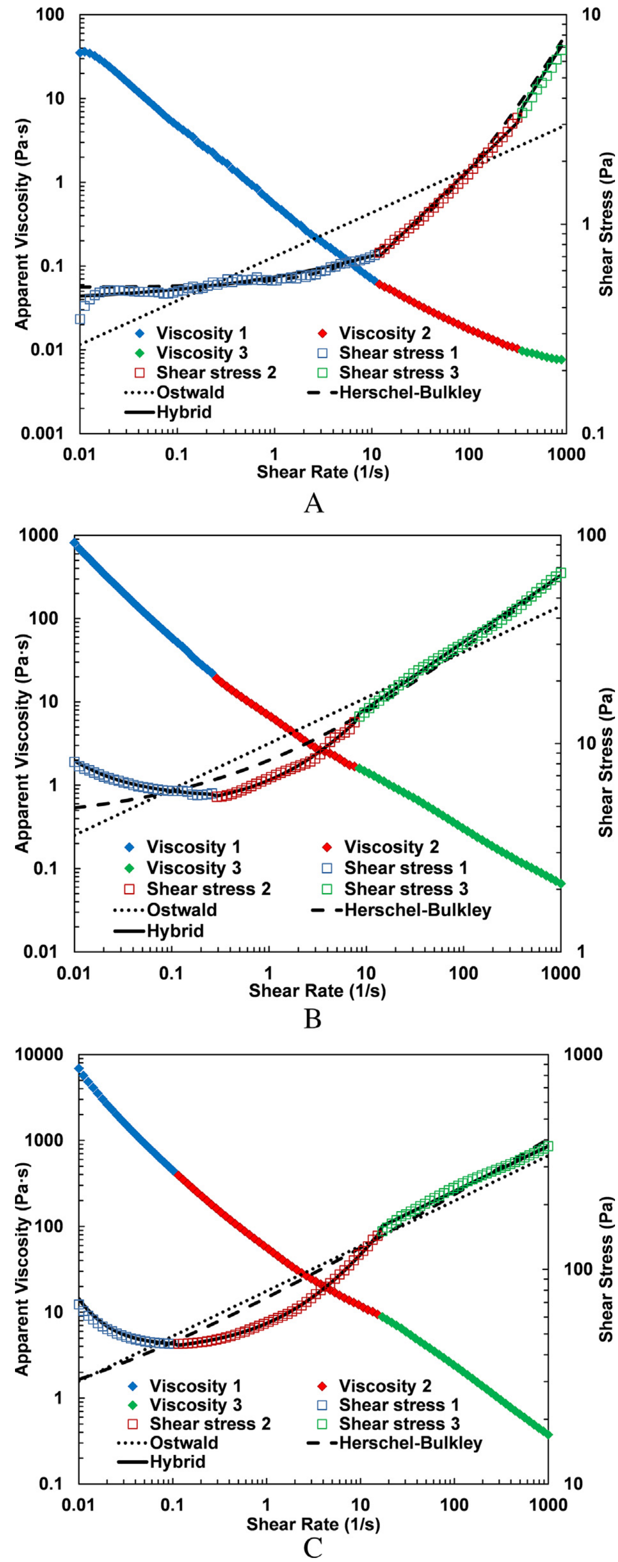


**Fig. 1.** Three distinct segments in the rheograms of A: TS 1.2%, B: TS 3.6% and C: TS 6.0%, and the fitting results of shear stress data.

**Table 2**
Fitting results of the sludge with three TS concentrations, using the Ostwald model and the Herschel-Bulkley model.

| TS (%) | Model | | K | n | $\tau_0$ | SSE | RMSE |
|---|---|---|---|---|---|---|---|
| 1.2 | Ostwald | Whole | 0.70 | 0.20 | | $8.8{\cdot}10^{2}$ | $2.9{\cdot}10^{0}$ |
| | | Segment 1 | 0.57 | 0.06 | | $8.2{\cdot}10^{1}$ | $1.2{\cdot}10^{0}$ |
| | | Segment 2 | 0.23 | 0.45 | | $2.8{\cdot}10^{-5}$ | $9.8{\cdot}10^{-4}$ |
| | | Segment 3 | 0.05 | 0.73 | | $8.8{\cdot}10^{-8}$ | $9.9{\cdot}10^{-5}$ |
| | Herschel-Bulkley | Whole | 0.04 | 0.74 | 0.49 | $2.4{\cdot}10^{-1}$ | $4.5{\cdot}10^{-2}$ |
| | | Segment 1 | 0.14 | 0.31 | 0.42 | $2.4{\cdot}10^{-2}$ | $2.0{\cdot}10^{-2}$ |
| | | Segment 2 | 0.08 | 0.63 | 0.39 | $7.4{\cdot}10^{-3}$ | $1.7{\cdot}10^{-2}$ |
| | | Segment 3 | 0.01 | 0.99 | 1.22 | $1.2{\cdot}10^{-2}$ | $4.4{\cdot}10^{-2}$ |
| 3.6 | Ostwald | Whole | 10.01 | 0.22 | | $5.9{\cdot}10^{5}$ | $7.7{\cdot}10^{1}$ |
| | | Segment 1 | 4.73 | −0.10 | | $5.3{\cdot}10^{3}$ | $1.4{\cdot}10^{1}$ |
| | | Segment 2 | 6.95 | 0.25 | | $3.6{\cdot}10^{0}$ | $3.5{\cdot}10^{-1}$ |
| | | Segment 3 | 7.10 | 0.32 | | $4.9{\cdot}10^{-3}$ | $1.1{\cdot}10^{-2}$ |
| | Herschel-Bulkley | Whole | 4.08 | 0.39 | 4.24 | $1.6{\cdot}10^{2}$ | $1.3{\cdot}10^{0}$ |
| | | Segment 1 | 0.06 | −0.83 | 5.52 | $6.5{\cdot}10^{-2}$ | $5.0{\cdot}10^{-2}$ |
| | | Segment 2 | 1.72 | 0.74 | 4.94 | $8.1{\cdot}10^{-1}$ | $1.7{\cdot}10^{-1}$ |
| | | Segment 3 | 3.91 | 0.39 | 5.83 | $1.7{\cdot}10^{1}$ | $6.6{\cdot}10^{-1}$ |
| 6.0 | Ostwald | Whole | 79.21 | 0.21 | | $3.6{\cdot}10^{7}$ | $6.0{\cdot}10^{2}$ |
| | | Segment 1 | 28.87 | −0.16 | | $6.9{\cdot}10^{5}$ | $1.8{\cdot}10^{2}$ |
| | | Segment 2 | 61.86 | 0.23 | | $1.1{\cdot}10^{4}$ | $1.6{\cdot}10^{1}$ |
| | | Segment 3 | 87.81 | 0.21 | | $6.0{\cdot}10^{-1}$ | $1.3{\cdot}10^{-1}$ |
| | Herschel-Bulkley | Whole | 60.56 | 0.27 | 13.24 | $2.4{\cdot}10^{4}$ | $1.6{\cdot}10^{1}$ |
| | | Segment 1 | 0.03 | −1.49 | 44.14 | $6.7{\cdot}10^{-1}$ | $1.9{\cdot}10^{-1}$ |
| | | Segment 2 | 14.87 | 0.71 | 41.16 | $1.0{\cdot}10^{1}$ | $5.1{\cdot}10^{-1}$ |
| | | Segment 3 | 90.80 | 0.21 | ~0 | $7.9{\cdot}10^{2}$ | $4.9{\cdot}10^{0}$ |

Although similar performances of the two models were obtained in some segments, the Herschel-Bulkley model was usually found to better describe the low shear rates (such as segment 1 of all, and segment 2 of the VFC sludge). On the other hand, the Ostwald model fit the data better at high shear rates (segment 3). The good performance of single model fitting in a specific shear rate range agreed with some previous results, but these studies also showed limitation of single model fitting, when applied in a wider shear rate range [17,23].

Hence, as shown in Fig. 1, to better characterise the varying rheological behaviour, hybrid model fitting was needed; the Herschel-Bulkley model at low shear rates and the Ostwald model at high shear rates were combined to describe the entire curve. It indicated that the role of yield stress reflected by the term ($\tau_0$) in the Herschel-Bulkley model was important at low shear rates, however, became less important and even negligible once reaching a high shear rate.

Moreover, two discrepancies in the regressed parameters should be noted in Table 2. Firstly, when the GT sludge (TS 1.2%) was fitted by the same model (Ostwald), segment 2 and 3 gave distinct K (0.23 and 0.05) and n (0.45 and 0.73) values, which seemed to express behaviour of two different types of sludge, rather than a transition. Secondly, when the same segment was fitted with Ostwald and Herschel-Bulkley, both models achieved an acceptable regression (segment 2 and 3, TS 1.2%). However, the predicted *K* and *n* values were different, even though having the same definition. Therefore, the discrepancies may highlight the empirical nature of both models, implying a transient rheological status rather than fixed physical properties.

### 3.2.2. Models with higher complexity

In addition to the existing models, more complex models (Eqs. 4–8) were used in order to identify if the rheological data could be more accurately predicted. The more complex models included more limiting parameters, such as zero-shear apparent viscosity ($\mu_0$) and infinite rate apparent viscosity ($\mu_\infty$). Fitting results applying these models are shown in Fig. 2 and Table S1. It was found that, even with some modifications, the increased complexity did not return satisfactory fitting quality, especially for the flow curves of the VFC sludge.

In order to improve the fitting performance, a new expression was developed that includes critical shear stress ($\tau_C$) and the coefficients *n*

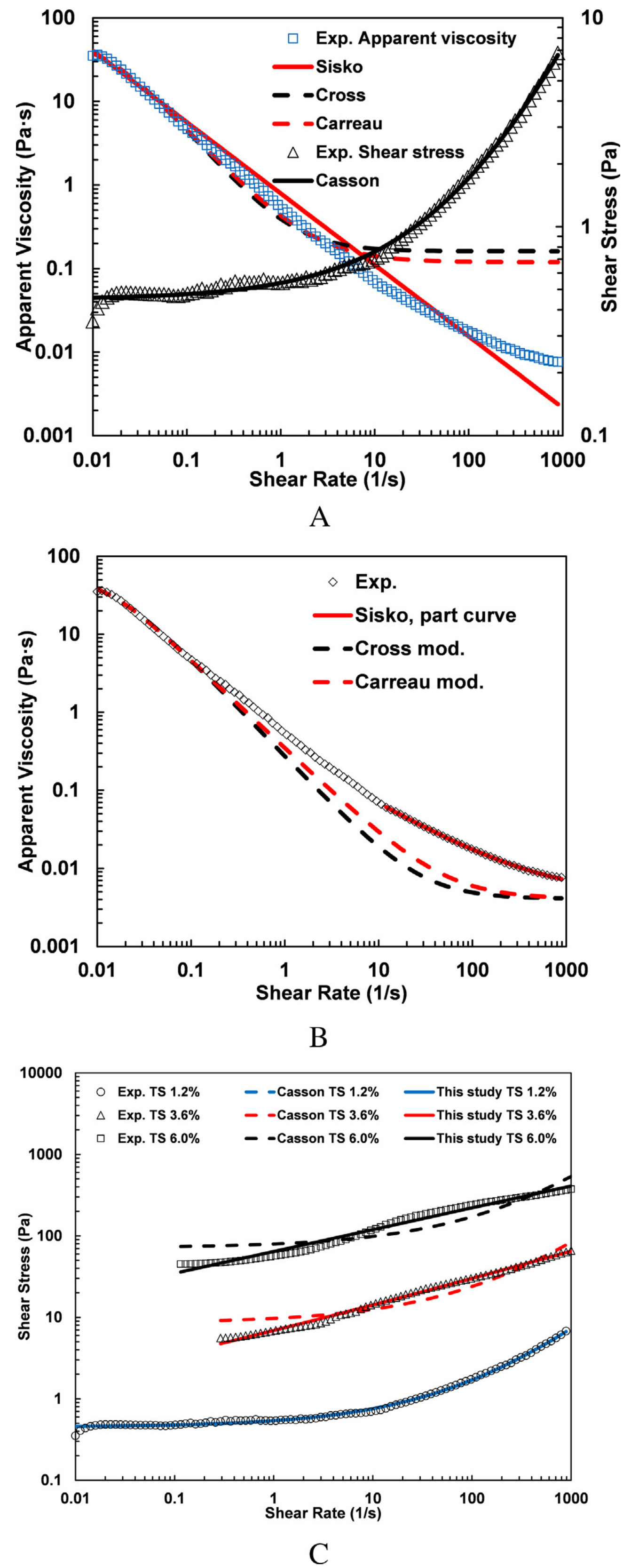


**Fig. 2.** Fitting by the models with limiting parameters, A: original and B: modified models for the GT sludge; and C: Casson and the expression in this study for the VFC sludge.

and $K_n$:

$$\sqrt{\tau} = \sqrt{\tau_C} + K_n\sqrt{\dot{\gamma}}^n \quad (9)$$

The fitting results of this expression in Table S1 and Fig. 2C demonstrate an improved fitting quality with much lower SSE and RMSE values than other models used. It seemed that the returned $K_n$ and $n$ were parameters similar to the $K$ and $n$ in Ostwald and Herschel-Bulkley, since consistent varying tendencies were obtained as TS increased. However, although close to yield stress ($\tau_0$) for the GT sludge, the critical shear stress ($\tau_C$) returned decreasing values at increasing TS, so this parameter seemed not only to be related to yield stress but also to TS. The proposed expression was applied to fit rheological data of other WAS, including thermophilic and mesophilic anaerobically digested sludge from WWTP Echten (The Netherlands, data not shown in this paper), showing improved fitting results as well. Therefore, considering the improvements of fitting quality, this empirically developed expression could be recommended to characterise the rheological behaviour of concentrated WAS in a wide shear rate range.

Moreover, it should be noted that verifying the theoretical $\mu_\infty$ by rheological measurements was very challenging in this study. For the GT sludge, the asymptote could not be extended further but showed an unreliable transition to shear-thickening (over $890\,s^{-1}$), which is further interpreted in Section 3.6. For the VFC sludge, a tendency to $\mu_\infty$ could not be found even at the upper shear stress limit of the applied rheometer (about $3800\,s^{-1}$). Hence, understanding the practical meaning of $\mu_\infty$ for concentrated sludge is unclear. It is also crucial for the applicability of the relevant rheological models, because an inaccurate prediction of $\mu_\infty$ could lead to assessment deviation of the minimum apparent viscosity in the strongest shear regions, e.g. when sludge is pumped or mixed in full-scale reactors.

The three TS concentrations investigated and described above were representative for all measured samples that are not shown here. Essentially, the employed segmentation was a method to improve the poor performance of characterising the total curves in a wide range of shear rates. The number of segments that needed to be applied for a decent description of the measurements was not universal and depended per sample, as can be seen from the different segments found with the GT and VFC sludge (Section 3.4). The inconsistency reflected in the model fitting indicated instable behaviour and changes of the sludge rheology at the specific applied shear rates.

### 3.3. Further characterisation of the rheological instability

In order to further confirm and characterise the instable rheological behaviour, more experimental approaches were applied for the varying trends and relevant transition parts in the flow curves, involved in both yielding and flowing status.

#### 3.3.1. Yielding process

Since the strict theoretical concept of yield stress is not yet clear [21] and debate still exists on the correct methodology [7,28], various methods were used to determine the sludge yield stress experimentally [3,10,29] or by applying different models [6,8,17,30]. In this study, different methods were assessed, determining $\tau_0$ by: (1) the initial point in a flow curve; (2) best model fitting (Herschel-Bulkley); (3) the linear range in a complex modulus curve from the dynamic oscillation measurement; and (4) the abrupt point in a deflection angle curve.

The data in Table 3 showed considerable discrepancies between the four methods, especially for the VFC sludge. With TS concentration over 3%, method 2 returned the lowest yield stress values, whereas method 4 showed the highest. The yield stress range determined by method 3 was close to method 1 for the VFC sludge (Table 3).

Method 1 could be used when the initial shear rate ($0.01\,s^{-1}$) approximated the yielding process. However, the decreasing shear stress trend indicated the possibility of underestimating the yield stress. Similar deviation was found in method 2, although it has been widely applied in previous research [6,8,17,30]. As indirect approaches, the estimated $\tau_0$ by methods 1 and 2 relies on the trend of the measured curve, similar to the limitation reported in literature [28]. Method 3 is a more direct approach by determining the critical shift of the sludge from "solid-like" to "liquid-like" at a certain oscillation frequency. However, as shown in Fig. 3A, the shift is smooth in each curve. Although not sharp enough, the obtained stress range was acceptable for the VFC sludge, which was also similar to literature values with comparable TS concentrations [3,10,26]. But method 3 was not suitable for the GT sludge, since an unacceptable high value was obtained. When assessing the rheological characteristics of the GT sludge, separation of flocs and supernatant was observed. Hence, instead of the original matrix, the more condensed sludge layer that was formed on the measuring plate may have accounted for the measured curve, which very likely led to a large overestimation of the yielding point.

Since the deflection angle represents the degree of sample deformation, method 4 is straightforward as well. Compared to method 3, the measured deflection angle had a precipitous increase to reflect the yielding process (Fig. 3B), with no risk of separation. The obtained $\tau_0$ is as expected and in line with the other methods. Therefore, method 4 is the best recommended approach to determine the yield stress for WAS. However, the discrepancies in the different methods also implied that the yielding was not a stable process and sensitive to shearing conditions.

#### 3.3.2. Distinct flow status

More rheological instability after yielding was revealed using a creep test. As shown in Fig. 4A, the responsive shear rate of the medium VFC sludge (TS 3.6%) decreased in time below the yielding point ($\le 8.0$ Pa). However, when the applied shear stress was over the yield stress, an instable flow status was obtained, showing fluctuations and a slightly decreasing averaged shear rate in time. A stable flow with a smooth plateau was achieved above 16 Pa, and thixotropic behaviour was found, since the shear rate kept increasing with time. Results of the corresponding shear strain shown in Fig. 4B were different with other studies [11,17]. The different critical stress found in this study could not be distinguished by the concave shape change of the curves of the sludge without thixotropy [17], or the asymptotic tendency formed in the sludge with comparable TS levels but much less viscoelasticity [11]. In addition, compared to the previous results [26], the larger magnitude of modulus also indicated stronger viscoelasticity in the studied WAS, resulting in more rheological transitions. The range of the critical transition to flow stability (14–16 Pa) covered the transition between segment 2 and 3 (14.1 Pa in Fig. 1B). The same comparison of the critical stress in different TS concentrations is shown in Table 4, indicating a good similarity between the results obtained from these

**Table 3**
Results of the yield stress (Pa) determined by four methods.

| TS (%) | 1 Initial point of flow curve | 2 Model fitting (Herschel-Bulkley) | 3 Dynamic oscillation measurement | 4 Deflection angle measurement |
|---|---|---|---|---|
| 1.2 | 0.4 | 0.4 | – | 0.4 |
| 1.5 | 0.5 | 0.6 | – | 0.5 |
| 1.6 | 0.2 | – | 12.0–15.6 | – |
| 2.5 | 3.5 | 4.2 | – | 2.9 |
| 3.6 | 7.8 | 5.5 | – | 8.2 |
| 4.2 | 17.8 | 10.5 | – | 19.7 |
| 4.5 | 22.6 | 14.4 | – | 24.4 |
| 4.6 | 41.3 | – | 43.0–50.1 | – |
| 6.0 ± 0.2* | 68.6 | 44.1 | – | 77.3 |
| 6.3 | 82.8 | – | 86.5–100.6 | – |
| 7.0 | 94.9 | 64.9 | – | 126.0 |

* The standard deviation of the other TS data was below 0.06%.

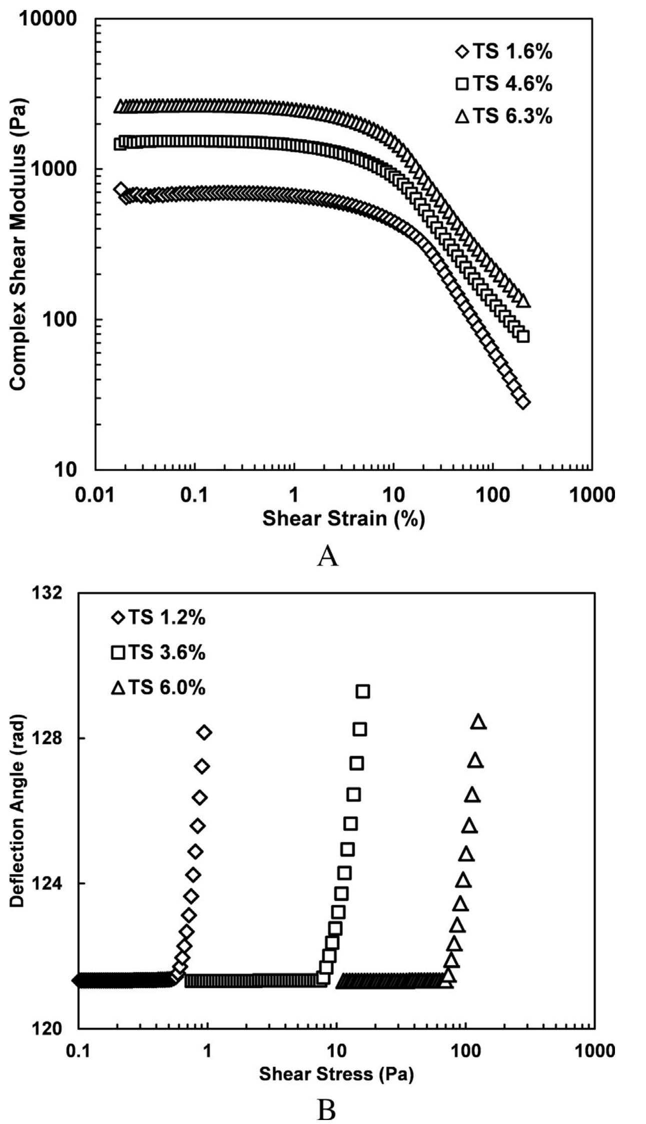


**Fig. 3.** Experimental results for determining the yield stress, A: the dynamic oscillation measurement, B: the deflection angle measurement.

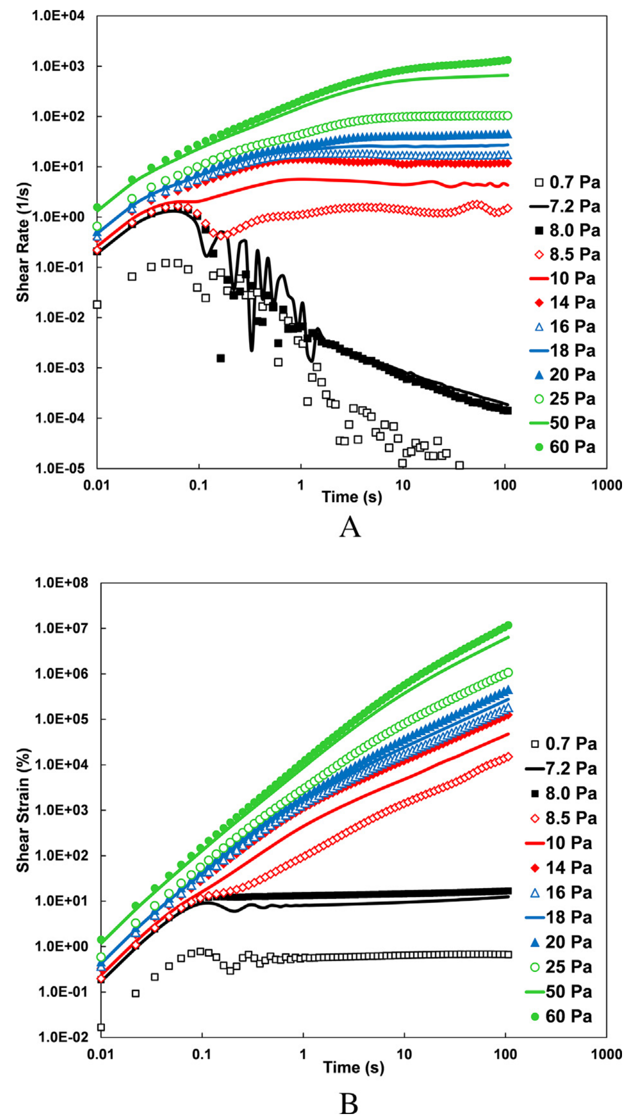


**Fig. 4.** Variation of A: responsive shear rate and B: shear strain in the creep tests (TS 3.6%).

methods. Therefore, the rheological instability was found not occasional or random, but can be revealed by using different methods, including experiments and model fitting.

### 3.3.3. Thixotropic behaviour

The thixotropic behaviour was further characterised by measuring in an increase-decrease shear mode (from 0 to 100 $s^{-1}$ and back to 0 again). The results shown in Fig. 5A demonstrated a larger hysteresis loop at higher TS concentrations, indicating a stronger influence on the rheology by shear time or shear history. Similar results were obtained when measuring sludge rheology in a membrane bioreactor, indicating that thixotropy was more apparent as the biomass concentration increased due to growth (up to 2%) [22]. Competition between solids interactions and viscous forces was reported to be responsible for thixotropy [18]. Moreover, flocs have been reported to have a re-flocculate ability; due to the physicochemical interactions between separated fragments, fractured flocs can reversibly form and even develop in larger sizes in stagnancy, leading to settling [15]. Hence, the dynamic floc structure in WAS could lead to these differences in the hysteresis loop. In the shear-increase step, large flocs would undergo breakage and deformation, which could not totally recover in time under durable shearing. Thus in the shear-decrease step, the overall bonding effect on the internal structure of the sludge will be weakened, leading to the hysteresis shown in Fig. 5A. Although nearly no hysteresis formed, thixotropy was still present in the GT sludge (TS 1.5%). As shown in Fig. 5B, once yielding was overcome, the flow status could be maintained by a shear stress (0.4 Pa) lower than the yield stress (> 0.5 Pa initially).

Therefore, subjecting WAS with considerable rheological instability to anaerobic digestion, requires insight in the conditional changes in practice. Especially in a system with high shear-rate gradients, applying a flow or mixing beyond yielding may not be enough, since an instable flow status may still exist below a critical shear rate level.

**Table 4**
Critical points of shear stress determined by different experimental methods.

| TS (%) | Yield stress (Pa) | | Shear stress of transition 2 (Pa) | |
|---|---|---|---|---|
| | Method 4 | Creep test | Flow curve | Creep test |
| 1.2 | 0.22 | 0.20–0.25 | 0.51 | 0.5–0.6 |
| 3.6 | 8.2 | 8.0–8.5 | 14.1 | 14–16 |
| 7.0 | 95 | 92–108 | 286 | 250–270 |

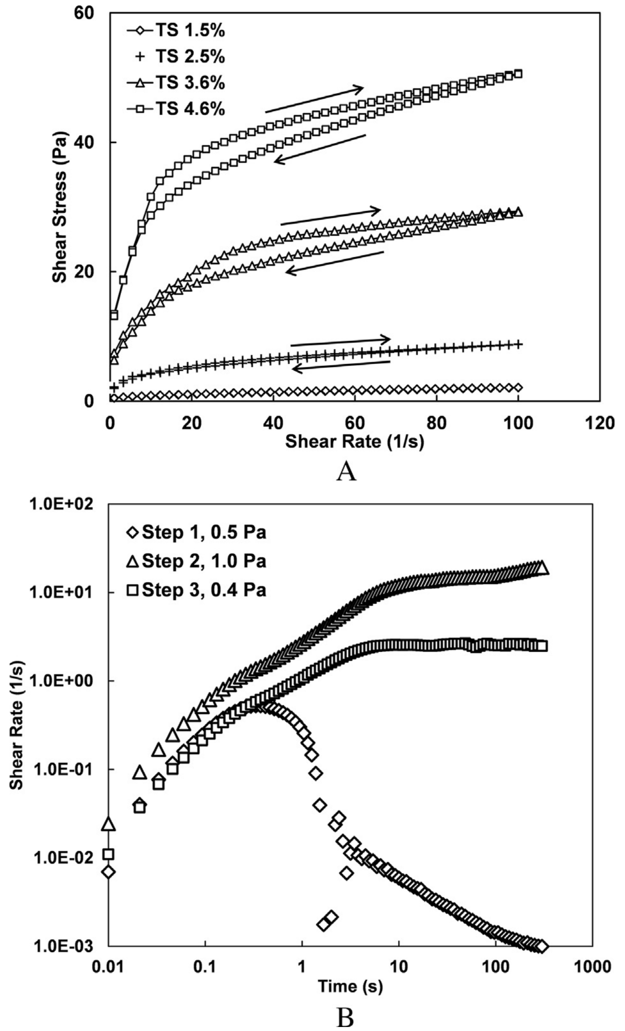


**Fig. 5.** Thixotropic behaviour of the WAS, A: hysteresis in sludge with different TS concentrations; B: time-dependent yielding of the GT sludge.

### *3.4. Total solids impact on the rheological instability*

As a key influencing factor on the rheological instability, the impact of the solids content was further investigated. As shown in Fig. 6, the correlation between yield stress and TS is better described as exponential in a TS range of 1–5%, which agrees with the previous studies [3,6,11,12]. However, when the TS range was extended to 7%, the yield stress would be overestimated by the exponential relation at the low TS part, whereas the power law relation described better. Hence, a proper correlation relied on the specific TS range taken into consideration. In addition, the increased normal stress from the sludge on the measuring bob also indicated a stronger force perpendicular to the shear stress as TS increased. Hence, the highly nonlinear increase in stress levels over 3% TS implied that the components in the sludge seem to build a 3D steric network for cohesion that becomes more strengthened at high TS concentrations.

More parameters for the rheological instability correlated to TS are shown in Table 5. For the VFC sludge, the critical shear rate for a stable flow (transition 2) increased more linearly to TS ($R^2$ 0.96); but decreased towards a constant level ($0.13\,s^{-1}$) for an instable flow (transition 1), indicating an enlarging instable flow range as TS increased.

For the GT sludge, the thixotropy was not strong enough to clearly show transition 1. However, the increasing $n$ in the different indicated segments suggested more 'Newtonian' behaviour as the shear rate increased. The increasing $K$ and decreasing $n$ obtained in the stable flow status (Segment B) agreed with expected behaviour: increased pseudoplastic at increased TS. However, in the instable flow status (Segment A), the $n$ got an abnormal value (> 1) and stayed almost constant (0.7) at TS above 3%, indicating an almost TS-independent level of the flow behaviour index in the low shear rates. Hence, more challenge was confronted to characterise the instable rheological status by the commonly used model fitting, since inconsistent and contradictory results were obtained. The weakened impact from TS on the rheological behaviour at low shear rates, also implied its dependency on the applied shear rate. Moreover, it could be perceived that for non-Newtonian WAS in a digester, the mixing performance difference resulting from the relevant shear rate difference, might be further enlarged by the TS difference on the long term.

### *3.5. Special rheological behaviour at low shear rates*

The decreasing shear stress part between the yielding point and transition 1, indicated strong instability caused by viscoelasticity and thixotropy, thus brought more uncertainty to be clearly determined. As discussed in Section 3.3.3, a flow status could be maintained by smaller shear stress after yielding, so it was possible to obtain the decreasing shear stress curve. A similar phenomenon was reported in the study of Pignon et al. [31], in which the flow pattern was visualised using a transparent colloidal suspension. Localised shear or stick slip was observed in the regime of decreasing shear stress: only part of the sample was activated as a shear layer when imposing quite low shear rates (even to $10^{-4}\,s^{-1}$). So, the sheared layer thickness $d_{eff}$ could be used to roughly calculate the effective shear rate using:

$$\dot{\gamma}_{eff} = \dot{\gamma}d/d_{eff} \quad (10)$$

where $\dot{\gamma}$ denotes the measured shear rate and $d$ the whole gap width. Based on this equation, the effective shear rate will be larger than the measured one if $d_{eff}$ is smaller than $d$. When calculating apparent viscosity,

$$\mu = \tau/\dot{\gamma} \quad (11)$$

this could result in an overestimation of the apparent viscosity and thus to abnormal regressed n values (in Table 2). So, the expected asymptote to theoretical $\mu_0$ at the very low shear rates might also be covered. An abrupt transition from flow towards stagnation was reported when measuring pasty sludge at high TS concentrations, also indicating that the effective shear was just covering a part of the whole gap [18]. Besides, the localised shear could be described in a non-monotonic pattern by a sandwich-like structure model, in which more specific parameters and expressions were used to determine the decreasing part [32]. Moreover, the region containing the minimum shear stress after

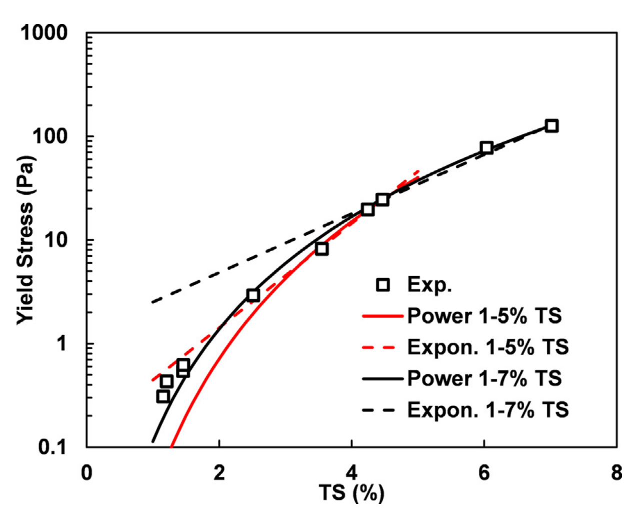


**Fig. 6.** Correlation between the measured yield stress and TS concentrations.

**Table 5**
Rheological instability of the sludge with various TS concentrations, characterised by three critical transitions and hybrid model fitting results.

| TS (%) | Transition 1 (shear rate, 1/s) | Segment A (instable flow status) | | Transition 2 (shear rate, 1/s) | Segment B (stable flow status) | | Transition 3 (shear rate, 1/s) | Segment C (stable flow status) | |
|---|---|---|---|---|---|---|---|---|---|
| | | *K* | *n* | | *K* | *n* | | *K* | *n* |
| 1.2 | – | 0.13 | 0.31 | 12.0 | 0.23 | 0.45 | 351.0 | 0.05 | 0.73 |
| 2.5 | 0.33 | 0.28 | 1.15 | 5.3 | 2.24 | 0.36 | – | – | – |
| 3.6 | 0.29 | 1.72 | 0.74 | 9.6 | 7.10 | 0.32 | – | – | – |
| 4.2 | 0.13 | 4.87 | 0.67 | 13.5 | 18.60 | 0.29 | – | – | – |
| 6.0 | 0.12 | 14.87 | 0.71 | 17.1 | 87.81 | 0.21 | – | – | – |
| 7.0 | 0.13 | 25.55 | 0.72 | 19.2 | 159.14 | 0.19 | – | – | – |

yielding showed an increasing thickness of the sheared layer. This behaviour was proposed as another critical shear condition (transition point 1 in Table 5) [32], below which the flow was extremely instable [33].

Although it seemed not feasible to visualise flow regions in the samples, potential localised shear or sandwich-like structures might account for the special behaviour. Furthermore, as discussed in Section 3.3.3, different to the colloidal suspension, the floc formation in WAS may also be an influencing factor. When overcome yielding, rupture of the dynamic floc structure may further loosen the connection between particles, which reduces the resistance to flow. In addition, the decreasing shear stress part was hardly observed in the measurement of digested sludge with similar TS concentrations (data not shown in this paper) compared to the fresh WAS, indicating that the related physicochemical interactions for the reversible floc formation might become weaker during the sludge aging process.

However, describing the decreasing part is more challenging than the other parts in the rheograms. Regarding the returned abnormal results ($n < 0$), an improved model with time-dependent functioning for thixotropy seems necessary. Moreover, due to thixotropy, the yielding underlying a simple value was dynamic and complicated in the studied WAS samples. Regarding design and operation in practice, the difficulty in estimating apparent viscosity at low shear rates, can bring more challenges for assessing and optimising the energy requirement when continuously pumping WAS, or for assessing the mixing performance in considerable low-shear regions distributed in digesters.

### 3.6. Suggestions on a proper protocol for rheological measurements

Although no standardised laboratory protocol has been established for sludge yet [7], it is necessary to develop a proper methodology for sludge with diverse behaviour. Hence, some recommendations can be given to improve the rheological measurements in a concentric rotational rheometer, especially for viscoplastic and thixotropic matrices.

#### 3.6.1. Determining the yield stress

The yield stress measurement should be straightforward, and carefully focused on the deformation of the sample whenever thixotropic behaviour is observed. In the present research, determining the abrupt changing point in a measured deflection angle curve was recognized as an effective method.

#### 3.6.2. Pre-shear step

Besides a homogeneous distribution of the sample, the rotational speed of pre-shear should not be too intense to further deform the sample structure, especially for thixotropic samples, since it could lead to an underestimation of the shear stress (Fig. 5). In literature, the opposite is advised as well [10,23,34–36], to apply high pre-shear rates to erase the material memory (or shear history) of the sludge. However, if the rest time is not long enough, this could lead to disruption of the sludge flocs and would therefore give a wrong impression of behaviour of sludge during low mixing conditions, e.g. flowing out of a sludge thickener, being pumped from a sludge buffer, or mixing in large scale digesters in the more stagnant or low mixing zones.

#### 3.6.3. Shear rate range in measurement

For concentric rotational rheometers, no distinct indication could be identified when the flow turns from laminar to turbulent [1]. However, when flow is not laminar, secondary flows (or Taylor-Couette instability) will be generated and lead to an incorrect shear-thickening result [2]. In order to avoid this transition, the Reynolds number (*Re*) or the Taylor number (*Ta*) needs to be estimated for each measurement. In Taylor-Couette flow, *Re*, critical *Re* to turbulent, and *Ta* can be calculated by using Eqs. (12–14) [37], respectively. The critical *Re* and *Ta* for Taylor vortex generation is usually around 145 and 1708, respectively [38].

$$Re = \omega R_i d/\upsilon \tag{12}$$

$$Re_{transition} = 41.3\sqrt{(R_i + R_o)/2d} \tag{13}$$

$$Ta = \omega^2 R_i d^3/\upsilon^2 \tag{14}$$

where $\omega$ denotes the angular velocity, $R_i$ the bob radius, $d$ the gap width and $\upsilon$ the kinematic viscosity of fluid. The *Re* (167.9) and *Ta* (2168) of the maximum shear rate point (1000 $s^{-1}$) in the GT sludge were found to be above the critical values, and the corresponding apparent viscosity was larger than the result at 890 $s^{-1}$. The point influenced by Taylor vortex generation could therefore be eliminated. Moreover, the maximum *Re* and *Ta* sharply decreased (41 and 144, respectively, TS 2.5%) into the laminar range as TS increased. Hence, *Re* or *Ta* should always be estimated to control the setting of shear rate range in laminar flow.

## 4. Conclusions

For the yield-pseudoplastic behaviour of the studied WAS, clear rheological characterisation depended on hybrid model fitting of defined shear rate segments. Although a new mathematical expression improved fitting quality, limited applicability of the empiric models reflected the samples' transient rheological behaviour rather than intrinsic properties, challenging the included parameters definition. Characterised by the distinct flow status and transitions, the rheological instability could give more insight in viscoelasticity and thixotropy, which impact sludge flow and mixing in full-scale WAS treatment systems. The observed rheological instability is more pronounced at increased TS concentrations, which are commonly found in WAS digesters.

## Declarations of interest

None.

## Acknowledgements

The authors appreciate the collaboration with Ir. Mark van den

Braak from De Groote Lucht WWTP (Vlaardingen, the Netherlands) for supplying sludge samples. China Scholarship Council (CSC) is acknowledged to support Peng Wei's PhD research at Delft University of Technology.

## Appendix A. Supplementary data

Supplementary data associated with this article can be found, in the online version, at http://dx.doi.org/10.1016/j.cej.2018.04.108.

## References


[1] I. Seyssiecq, J.-H. Ferrasse, N. Roche, State-of-the-art: rheological characterisation of wastewater treatment sludge, Biochem. Eng. J. 16 (2003) 41–56.

[2] N. Ratkovich, W. Horn, F.P. Helmus, S. Rosenberger, W. Naessens, I. Nopens, T.R. Bentzen, Activated sludge rheology: a critical review on data collection and modelling, Water Res. 47 (2013) 463–482.

[3] M. Mori, I. Seyssiecq, N. Roche, Rheological measurements of sewage sludge for various solids concentrations and geometry, Process Biochem. 41 (2006) 1656–1662.

[4] I. Seyssiecq, B. Marrot, D. Djerroud, N. Roche, In situ triphasic rheological characterisation of activated sludge, in an aerated bioreactor, Chem. Eng. J. 142 (2008) 40–47.

[5] V. Lotito, L. Spinosa, G. Mininni, R. Antonacci, The rheology of sewage sludge at different steps of treatment, Water Sci. Technol. 36 (1997) 79–85.

[6] G. Guibaud, P. Dollet, N. Tixier, C. Dagot, M. Baudu, Characterisation of the evolution of activated sludges using rheological measurements, Process Biochem. 39 (2004) 1803–1810.

[7] N. Eshtiaghi, F. Markis, S.D. Yap, J.-C. Baudez, P. Slatter, Rheological characterisation of municipal sludge: a review, Water Res. 47 (2013) 5493–5510.

[8] G. Moeller, L.G. Torres, Rheological characterization of primary and secondary sludges treated by both aerobic and anaerobic digestion, Bioresour. Technol. 61 (1997) 207–211.

[9] S. Baroutian, N. Eshtiaghi, D.J. Gapes, Rheology of a primary and secondary sewage sludge mixture: dependency on temperature and solid concentration, Bioresour. Technol. 140 (2013) 227–233.

[10] J.-C. Baudez, R.K. Gupta, N. Eshtiaghi, P. Slatter, The viscoelastic behaviour of raw and anaerobic digested sludge: strong similarities with soft-glassy materials, Water Res. 47 (2013) 173–180.

[11] F. Markis, J.-C. Baudez, R. Parthasarathy, P. Slatter, N. Eshtiaghi, Rheological characterisation of primary and secondary sludge: impact of solids concentration, Chem. Eng. J. 253 (2014) 526–537.

[12] F. Markis, J.-C. Baudez, R. Parthasarathy, P. Slatter, N. Eshtiaghi, The apparent viscosity and yield stress of mixtures of primary and secondary sludge: impact of volume fraction of secondary sludge and total solids concentration, Chem. Eng. J. 288 (2016) 577–587.

[13] L.H. Mikkelsen, The shear sensitivity of activated sludge: relations to filterability, rheology and surface chemistry, Colloids Surf., A 182 (2001) 1–14.

[14] F.D. Sanin, Effect of solution physical chemistry on the rheological properties of activated sludge, Water SA 28 (2002) 207–211.

[15] B. Jin, B.M. Wilen, P. Lant, A comprehensive insight into floc characteristics and their impact on compressibility and settleability of activated sludge, Chem. Eng. J. 95 (2003) 221–234.

[16] S.N. Bhattacharya, Flow characteristics of primary and digested sewage sludge, Rheol. Acta 20 (1981) 288–298.

[17] J.C. Baudez, P. Coussot, Rheology of aging, concentrated, polymeric suspensions: application to pasty sewage sludges, J. Rheol. 45 (2001) 1123–1139.

[18] J.C. Baudez, Physical aging and thixotropy in sludge rheology, Appl. Rheol. 18 (2008) 8.

[19] N. Tixier, G. Guibaud, M. Baudu, Determination of some rheological parameters for the characterization of activated sludge, Bioresour. Technol. 90 (2003) 215–220.

[20] B.-H. Chen, S.-J. Lee, D.J. Lee, Rheological characteristics of the cationic polyelectrolyte flocculated wastewater sludge, Water Res. 39 (2005) 4429–4435.

[21] R.P. Chhabra, J.F. Richardson, Non-Newtonian Flow and Applied Rheology: Engineering Applications, Butterworth-Heinemann, Oxford, 2008.

[22] A. Pollice, C. Giordano, G. Laera, D. Saturno, G. Mininni, Physical characteristics of the sludge in a complete retention membrane bioreactor, Water Res. 41 (2007) 1832–1840.

[23] J.C. Baudez, F. Markis, N. Eshtiaghi, P. Slatter, The rheological behaviour of anaerobic digested sludge, Water Res. 45 (2011) 5675–5680.

[24] N. Eshtiaghi, S.D. Yap, F. Markis, J.-C. Baudez, P. Slatter, Clear model fluids to emulate the rheological properties of thickened digested sludge, Water Res. 46 (2012) 3014–3022.

[25] H. Tabuteau, P. Coussot, J. Baudez, A new approach to the thixotropic behaviour of sewage sludge, J. Residuals Sci. Technol. 3 (2006) 233–240.

[26] E. Farno, J.C. Baudez, R. Parthasarathy, N. Eshtiaghi, The viscoelastic characterisation of thermally-treated waste activated sludge, Chem. Eng. J. 304 (2016) 362–368.

[27] APHA, Standard Methods for the Examination of Water and Wastewater, 22nd ed., American Public Health Association, American Water Works Association, Water Environment Federation, Washington, 2012.

[28] M. Hannote, F. Flores, L. Torres, E. Galindo, Apparent yield stress estimation in xanthan gum solutions and fermentation broths using a low-cost viscometer, Chem. Eng. J. 45 (1991) B49–B56.

[29] L. Spinosa, V. Lotito, A simple method for evaluating sludge yield stress, Adv. Environ. Res. 7 (2003) 655–659.

[30] P.T. Slatter, The rheological characterisation of sludges, Water Sci. Technol. 36 (1997) 9–18.

[31] F. Pignon, A. Magnin, J.M. Piau, Thixotropic colloidal suspensions and flow curves with minimum: identification of flow regimes and rheometric consequences, J. Rheol. 40 (1996) 573–587.

[32] P. Coussot, A.I. Leonov, J.M. Piau, Rheology of concentrated dispersed systems in a low molecular weight matrix, J. Nonnewton. Fluid Mech. 46 (1993) 179–217.

[33] P. Coussot, Q.D. Nguyen, H.T. Huynh, D. Bonn, Viscosity bifurcation in thixotropic, yielding fluids, J. Rheol. 46 (2002) 573–589.

[34] J.C. Baudez, P. Slatter, N. Eshtiaghi, The impact of temperature on the rheological behaviour of anaerobic digested sludge, Chem. Eng. J. 215–216 (2013) 182–187.

[35] E. Farno, J.C. Baudez, R. Parthasarathy, N. Eshtiaghi, Rheological characterisation of thermally-treated anaerobic digested sludge: impact of temperature and thermal history, Water Res. 56 (2014) 156–161.

[36] E. Farno, J.C. Baudez, R. Parthasarathy, N. Eshtiaghi, Impact of temperature and duration of thermal treatment on different concentrations of anaerobic digested sludge: kinetic similarity of organic matter solubilisation and sludge rheology, Chem. Eng. J. 273 (2015) 534–542.

[37] F.M. White, Fluid Mechanics, McGraw-Hill, New York, 2011.

[38] P.G. Drazin, W.H. Reid, Hydrodynamic Stability, Cambridge University Press, Cambridge, 2004.